Hindawi Publishing Corporation
Journal of Nanomaterials
Volume 2016, Article ID 5121572, 6 pages
http://dx.doi.org/10.1155/2016/5121572

Research Article

A Self-Powered Triboelectric Nanosensor for PH Detection

Ying Wu,[1] Yuanjie Su,[2] Junjie Bai,[1] Guang Zhu,[3] Xiaoyun Zhang,[1] Zhanolin Li,[1] Yi Xiang,[1] and Jingliang Shi[1]

[1] *Chongqing University of Science and Technology, Chongqing 401331, China*
[2] *State Key Laboratory of Electronic Thin Films and Integrated Devices, School of Optoelectronic Information, University of Electronic Science and Technology of China (UESTC), Chengdu 610054, China*
[3] *Beijing Institute of Nanoenergy and Nanosystems, Chinese Academy of Sciences, Beijing 100083, China*

Correspondence should be addressed to Jingliang Shi; shijingliangcq@126.com

Received 21 August 2015; Accepted 19 January 2016

Academic Editor: Owen J. Guy

A self-powered, sliding electrification based triboelectric sensor was developed for detecting PH value from a periodic contact/separation motion. This innovative, cost-effective, simply designed sensor is composed of a fluorinated ethylene propylene thin film and an array of electrodes underneath. The operation of the TENG (triboelectric nanogenerator) sensor relies on a repetitive emerging-submerging process with traveling solution waves, in which the coupling between triboelectrification and electrostatic induction gives rise to alternating flows of electrons between electrodes. On the basis of coupling effect between triboelectrification and electrostatic induction, the sensor generates electric output signals which are associated with PH value. Experimental results show that the output voltage of the TENG sensor increases with the increasing PH value, which indicate that the PH value of different solution can be real-time monitored. This work not only demonstrates a new principle in the field of PH value measurement but also greatly expands the applicability of triboelectric nanogenerator (TENG) as self-powered sensors.

1. Introduction

As one of the analytical devices, pH sensors play an important role in many fields such as environment monitors, biological analyses, blood monitors, and medical detection [1]. Over the past decade, major advances have occurred in PH measurement based on electrochemical effects, such as modification of nanostructured pH sensing electrodes [2] and doping of nanostructured single electrode of electrochemical sensors [3]. However, widespread usage of these techniques is likely to be shadowed by possible limitations, including structure complexity, requirement of sophisticated materials, and reliance on external power source. Recently, triboelectric nanogenerator [4–10], creative invention based on the coupling of the universally known contact electrification effect and electrostatic induction, has been extensively explored to establish cost-effective and robust self-powered sensing systems, including but not limited to vibration sensor [11], motion sensor [12], acoustic sensor [13], biosensor [14], displacement vector sensor [15], acceleration sensor [16], wind vector sensor [17], tactile sensor [18], tracking sensor [19], and chemical sensor [20, 21]. Here, based on the previous research of harvesting water wave energy with TENG [22], we, for the first time, introduce a new principle in PH detection by fabricating a triboelectric sensor. The as-fabricated self-powered sensor is based on a periodic contact/separation between PH solution and a fluorinated ethylene propylene (FEP) film. The ions of the buffer solution with different PH value induced variation in surface potential are readily measured as a change in triboelectric voltage of the TENG sensor. Triggered by the output voltage signal, the PH value of the buffer solution can be real-time monitored. This work not only presents a new principle in the field of PH measurement but also greatly expands the applicability of TENGs as power self-powered sensors.

2. Results and Discussion

The presented self-powered PH sensor has a fork-finger structure, which is shown in Figure 1(a). On one side of

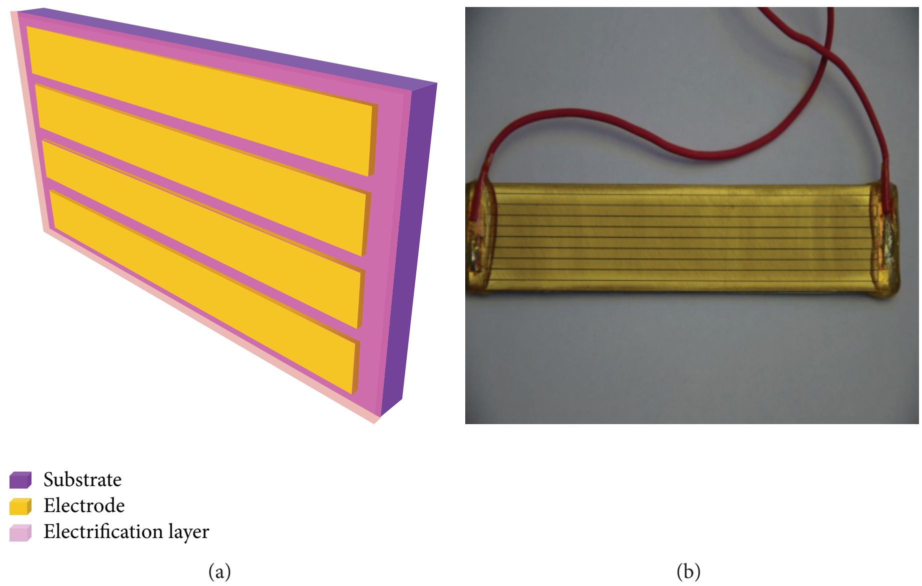

Figure 1: Structural design of the TENG sensor. (a) Schematic diagram of the fabricated sensor. (b) Photograph of the prepared TENG sensor.

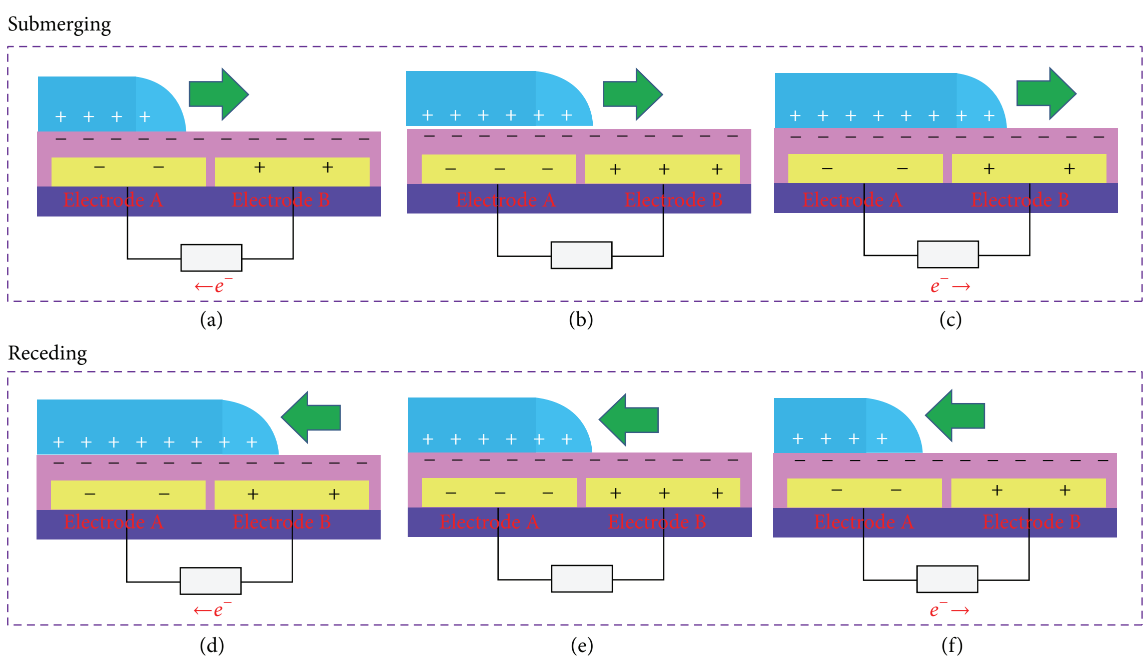

Figure 2: Working mechanism of the fabricated TENG sensor. (a) Electrode A is partially submerged. (b) The water surface levels with the middle point of the device. (c) Electrode B is being covered by water, (d) electrode B is partially exposed, (d) electrode B is completely exposed, and (f) electrode A is partially exposed.

a fluorinated ethylene propylene (FEP) thin film, four parallel strip-shaped electrodes are fabricated, which are discrete with a fine gap in between, as well as polyethylene terephthalate (PET) as the substrate. FEP is selected as the contact material for its hydrophobic property and high negativity in the triboelectric series [23]. As the area of the device submerged cyclically varies with the wave, free electrons are driven to flow alternatingly between electrodes, generating AC output electricity on the external load.

The operation of the TENG sensor involves a repetitive emerging-submerging process with traveling solution waves, which result in the coupling between triboelectrification and electrostatic induction between the TENG sensor and solution buffer and thus give rise to alternating flows of electrons. The electricity-generating process is described through a basic unit in Figure 2. We define the initial state (Figure 2(a)) and the final state (Figure 2(f)) as the states when the buffer solution is submerged with the bottom first-electrode area

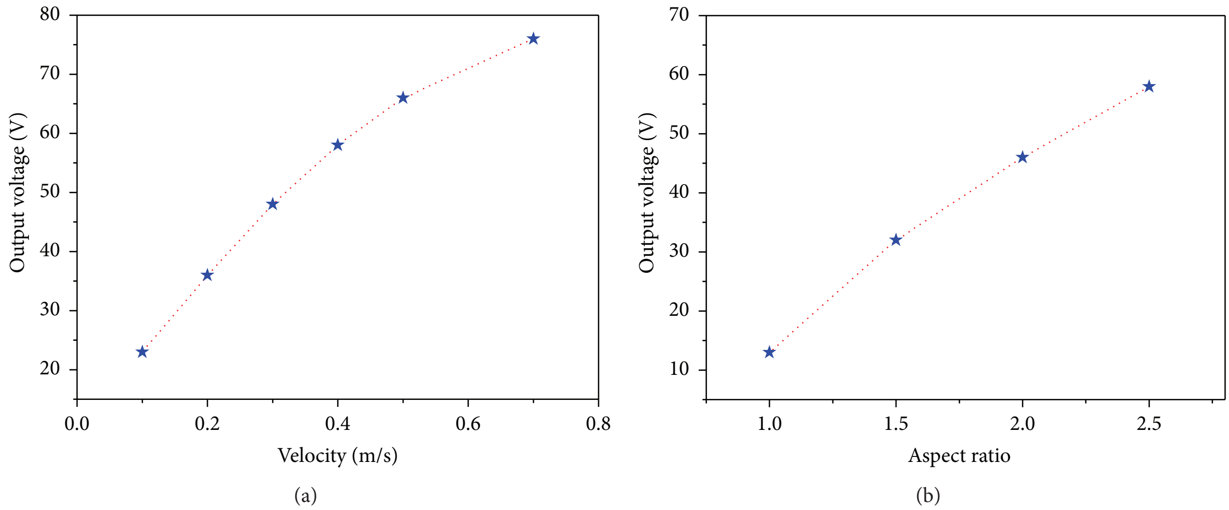

FIGURE 3: Electric measurement results of factors that influence the electric output. (a) Open-circuit voltage with increasing velocity. (b) Open-circuit voltage with increasing aspect ratio of the device.

and receded away from the bottom electrodes, respectively. The contact electrification between triboelectrically negative materials and solution renders the negative triboelectric charges on the surface of FEP thin film (Figure 2(a)). These surface charges can remain for a long period of time due to the insulating property of the polymer material [24]. When electrode A is increasingly submerged by the rising solution wave, positive ions in solution are attracted by the negative triboelectric charges on the FEP surface to form an interfacial electrical double layer (EDL). This asymmetric distribution of charges on FEP surface establishes the positive electric potential difference from electrode A to electrode B, driving electrons to flow from electrode B to electrode A (Figure 2(a)). Once the rising buffer solution reaches the gap between two electrodes, a maximum quantity of induced charges on the electrodes will be attained, leaving no electrons transferred (Figure 2(b)). As the rising water continues to submerge electrode B (Figure 2(c)), induced electrons flow back to electrode B since the electric potential difference between the two electrodes decreases until electrode B is fully submerged by buffer solution (Figure 2(c)). When the device is completely covered by buffer solution, a symmetric screening of triboelectric charges is achieved, and therefore the electric potential difference decreases to zero with no electrons transfer between electrodes. Then the wave begins to recede and expose electrode B and, thereby, the increasing electric potential difference drives electrons to flow from electrode B to electrode A (Figure 2(d)). Once the solution surface returns to the gap between two electrodes, a maximum quantity of induced charges on the electrodes will be obtained again without electron flowing (Figure 2(e)). Subsequently, the solution level falls down and exposes electrode A and the decreasing screening area results in electron flow from electrode A to electrode B (Figure 2(f)). Finally, the TENG sensor fully emerges from buffer solution and completes a whole cycle. The hydrophobic surface of FEP thin film repels solution immediately after emerging from solution surface. Consequently, as the device submerges and emerges from the waving solution, two pairs of alternating electron flows are brought about between the two adjacent electrodes, leading to power generation and outputting the corresponding signal, which can indicate the PH value of buffer solution.

In the previous research, nanowire-based modification from polymer nanowires plays a key role in increasing the output power [22]. However, nanowire-based modification is not very good for the PH detection. Here, the electric output of the sensor was improved by investigating two factors, that is, velocity of the relative movement and aspect ratio of the device. For TENG, the velocity is an important factor. The bigger the velocity was, the more the kinetic energy was produced and thus more triboelectric charges were generated on the FEP surface. As shown in Figure 3(a), the output voltage V_{oc} has an approximately linear relationship with the velocity. The induced voltage increases as the velocity increases from 0.1 to 0.7 m/s, which was similar to the previous studies on electrification between a fluorinated polymer and water [23, 24]. At the same time, the aspect ratio of the device is another important parameter that has a decisive effect on the electric output of the TENG sensor. Previous studies reported that preexisting charges in the solution can influence subsequent charge transfer with a solid surface [25, 26]. In order to optimize the aspect ratio, the TENG sensor was driven by a linear motor in a fixed velocity. When the TENG sensors do the reciprocating motion in the solution, the charge resulting from triboelectrification will transfer between the surface part of the solution and the TENG surface. Once the TENG starts to dip into the buffer solution, the surface part of the solution is positively charged instantaneously. As the TENG continues to dip into the buffer solution, preexisting positive charges in the solution will be increased thus decreasing the electrification. The more the area of the TENG sensor that will be submerged into the solution, the weaker the electrification that will be produced.

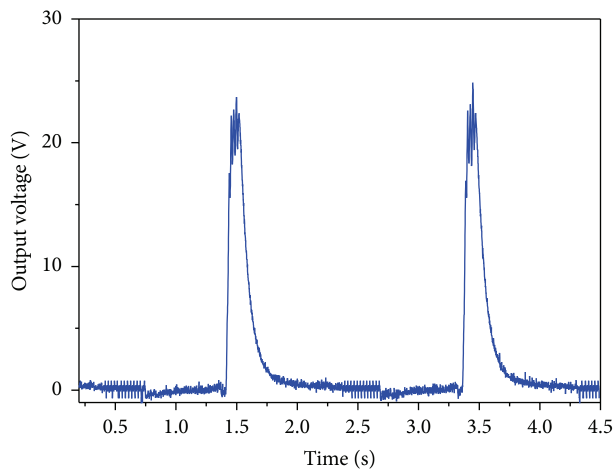

Figure 4: Open-circuit voltage results as the TENG is repetitively submerged into buffer solution.

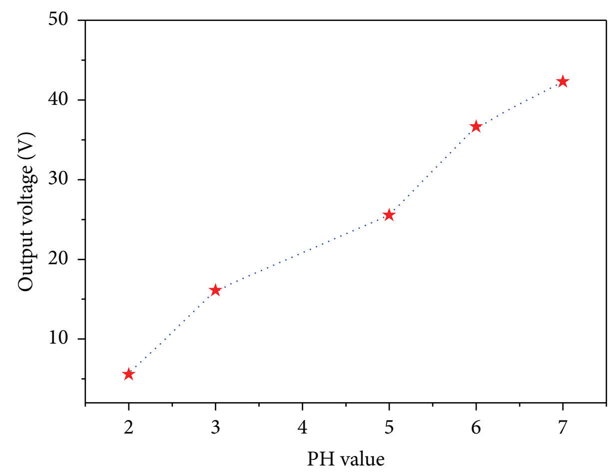

Figure 5: Relationship between output voltage and PH value.

Compared to the bottom part, the top part of the TENG may own a lower surface charging density.

For the fixed TENG surface area, more surface triboelectric charges and thus higher electric output will be produced accordingly for a narrower TENG with a higher aspect ratio has a shorter interaction distance with the solution, which was illustrated by the increasing V_{oc} in Figure 3(b). Therefore, according to the relationship between the electric output and the aspect ratio, the optimized size of the electrode and the TENG sensor with high performance will be achieved.

To demonstrate applications of the TENG for self-powered PH measurement, we mounted the sensor onto the linear motor to ensure reciprocating motion through the motor-controlling program for monitoring the PH value of the container in real-time.

Figure 4 shows the open-circuit output voltage of self-powered PH sensor. Here, the open-circuit voltage (V_{oc}) was defined as the electric potential difference between the two electrodes and the TENG sensors do the reciprocating motion in the buffer solution. In open-circuit condition, electrons cannot transfer between electrodes. When the TENG sensor submerged into the buffer solution, the open-circuit voltage is about 0 V. When the TENG sensor emerged from the buffer solution, the open-circuit voltage is also about 0 V. When the solution surface levels attain the middle point of the TENG sensor, the open-circuit voltage reaches the maximum.

The buffer solution was driven by linear motor mounted with the TENG sensor to form a repeated wave motion. According to the measurement results plotted in Figure 5, the output of TENG sensor is associated with the PH value. The output voltage increases with the increasing PH value. This result indicates that the output voltages of the TENG sensor are affected by the electrolytes in solution. This is due to the fact that FEP film cannot completely eliminate the adhesion of solution droplet after it emerges from solution. The residual electrolytical solution, including positive dissolved ions, remains on the surface and will partially screen the triboelectric charges on the FEP film, reducing the electrostatic induction and thus the electric output [26]. A low positive ion (H^+) concentration assists generation of the triboelectric charges, while a high concentration has the opposite effect [21]. The buffer solution with lower PH value indicates more H^+ concentration and renders more positive ions in electrolytical solution.

3. Conclusions

In summary, a self-powered sensor for PH measurement using triboelectrification was firstly demonstrated. The sensor has a fork-finger structure composed of FEP material and metal electrodes, as well as PET as the substrate. The reciprocating motion between TENG sensor and buffer solution leads to charge transfer between the adjacent Cu bottom electrodes, generating AC voltage in the external circuit. The output voltage of the TENG sensor varies with the buffer solution with different PH value due to the different ion concentration. And the PH value of buffer solution can be actively monitored in real-time by reading the output voltage. This work not only presents a new principle in the field of PH measurement but also greatly expands the applicability of TENGs as self-powered sensors. The electricity was generated through triboelectric effect at the solid-liquid interface upon directly interacting with ambient buffer solution, showing a practically feasible technology for water quality monitoring and environment protection.

4. Experimental Section

4.1. Fabrication of a TENG Sensor. A 1.5 mm thick acrylic sheet was cut into a hollow mask by precision laser cutting. The patterns in the mask were the same as electrodes. Then the mask was mounted onto the FEP film. The Cu layer was deposited onto the exposed PET surface by physical vapour deposition (PVD) to prepare the parallel electrode. Lead wires were connected to the electrodes as output terminals with one-to-one correspondence. Subsequently, a 75 mm thick FEP film was attached to the PET substrate.

4.2. Experimental Setup for Electric Measurement. TENG sensor was mounted vertically on the electrical linear motor. The sheet was immersed into the different PH buffer solution and perpendicular to the solution surface. The moving direction of the motor was perpendicular to the array of strip-shaped electrodes. A container filled with buffer solution was placed under the device with the water level adjacent to the device edge. The reciprocating motion of the TENG sensor was achieved through the motor-controlling program. The reciprocating motion of the linear motor forms waves of tap solution in the container. The output leads of TENG sensor were connected to Keithly 6514.

Conflict of Interests

The authors declare no competing financial interest.

Authors' Contribution

Ying Wu and Yuanjie Su contributed equally to this work.

Acknowledgments

This work was supported in part by the Research Foundation of Chongqing Municipal Education Committee (Grant no. KJ1401333) and Research Foundation of Chongqing University of Science & Technology (Grant no. CK2011Z08 and Grant no. CK2011Z09).

References

[1] S. Zhuiykov, "Solid-state sensors monitoring parameters of water quality for the next generation of wireless sensor networks," *Sensors and Actuators B: Chemical, Sensors and Actuators B*, vol. 161, no. 1, pp. 1–20, 2012.

[2] B. Xu and W.-D. Zhang, "Modification of vertically aligned carbon nanotubes with RuO_2 for a solid-state pH sensor," *Electrochimica Acta*, vol. 55, no. 8, pp. 2859–2864, 2010.

[3] R. Zhao, M. Xu, J. Wang, and G. Chen, "A pH sensor based on the TiO_2 nanotube array modified Ti electrode," *Electrochimica Acta*, vol. 55, no. 20, pp. 5647–5651, 2010.

[4] Z. L. Wang, "Triboelectric nanogenerators as new energy technology for self-powered systems and as active mechanical and chemical sensors," *ACS Nano*, vol. 7, no. 11, pp. 9533–9557, 2013.

[5] F.-R. Fan, Z.-Q. Tian, and Z. L. Wang, "Flexible triboelectric generator," *Nano Energy*, vol. 1, no. 2, pp. 328–334, 2012.

[6] G. Zhu, C. Pan, W. Guo et al., "Triboelectric-generator-driven pulse electrodeposition for micropatterning," *Nano Letters*, vol. 12, no. 9, pp. 4960–4965, 2012.

[7] G. Zhu, Z.-H. Lin, Q. Jing et al., "Toward large-scale energy harvesting by a nanoparticle-enhanced triboelectric nanogenerator," *Nano Letters*, vol. 13, no. 2, pp. 847–853, 2013.

[8] S. Wang, Y. Xie, S. Niu, L. Lin, and Z. L. Wang, "Freestanding triboelectric-layer-based nanogenerators for harvesting energy from a moving object or human motion in contact and non-contact modes," *Advanced Materials*, vol. 26, no. 18, pp. 2818–2824, 2014.

[9] L. Lin, Y. N. Xie, S. H. Wang et al., "Triboelectric active sensor array for self-powered static and dynamic pressure detection and tactile imaging," *ACS Nano*, vol. 7, no. 9, pp. 8266–8274, 2013.

[10] Y. J. Su, Y. Yang, H. L. Zhang et al., "Enhanced photodegradation of methyl orange with TiO_2 nanoparticles using a triboelectric nanogenerator," *Nanotechnology*, vol. 24, Article ID 295401, 2013.

[11] Q. J. Liang, Z. Zhang, X. Q. Yan et al., "Functional triboelectric generator as self-powered vibration sensor with contact mode and non-contact mode," *Nano Energy*, vol. 14, pp. 209–216, 2015.

[12] X. N. Xia, G. L. Liu, H. Y. Guo, Q. Leng, C. G. Hu, and Y. Xi, "Honeycomb-like three electrodes based triboelectric generator for harvesting energy in full space and as a self-powered vibration alertor," *Nano Energy*, vol. 15, pp. 766–775, 2015.

[13] J. Yang, J. Chen, Y. Liu, W. Yang, Y. Su, and Z. L. Wang, "Triboelectrification-based organic film nanogenerator for acoustic energy harvesting and self-powered active acoustic sensing," *ACS Nano*, vol. 8, no. 3, pp. 2649–2657, 2014.

[14] S. Wang, L. Lin, and Z. L. Wang, "Triboelectric nanogenerators as self-powered active sensors," *Nano Energy*, vol. 11, pp. 436–462, 2015.

[15] C. Bao Han, C. Zhang, X. H. Li et al., "Self-powered velocity and trajectory tracking sensor array made of planar triboelectric nanogenerator pixels," *Nano Energy*, vol. 9, pp. 325–333, 2014.

[16] Y. K. Pang, X. H. Li, M. X. Chen, C. B. Han, C. Zhang, and Z. L. Wang, "Triboelectric nanogenerators as a self-powered 3D acceleration sensor," *ACS Applied Materials & Interfaces*, vol. 7, no. 34, pp. 19076–19082, 2015.

[17] Z.-H. Lin, G. Cheng, Y. Yang, Y. S. Zhou, S. Lee, and Z. L. Wang, "Triboelectric nanogenerator as an active UV photodetector," *Advanced Functional Materials*, vol. 24, no. 19, pp. 2810–2816, 2014.

[18] Y. Yang, H. L. Zhang, X. D. Zhong et al., "Electret film-enhanced triboelectric nanogenerator matrix for self-powered instantaneous tactile imaging," *ACS Applied Materials and Interfaces*, vol. 6, no. 5, pp. 3680–3688, 2014.

[19] Y. Su, G. Zhu, W. Yang et al., "Triboelectric sensor for self-powered tracking of object motion inside tubing," *ACS Nano*, vol. 8, no. 4, pp. 3843–3850, 2014.

[20] C. Xu, C. Pan, Y. Liu, and Z. L. Wang, "Hybrid cells for simultaneously harvesting multi-type energies for self-powered micro/nanosystems," *Nano Energy*, vol. 1, no. 2, pp. 259–272, 2012.

[21] Y. C. Wu, X. D. Zhong, X. Wang, Y. Yang, and Z. L. Wang, "Hybrid energy cell for simultaneously harvesting wind, solar, and chemical energies," *Nano Research*, vol. 7, no. 11, pp. 1631–1639, 2014.

[22] G. Zhu, Y. Su, P. Bai et al., "Harvesting water wave energy by asymmetric screening of electrostatic charges on a nanostructured hydrophobic thin-film surface," *ACS Nano*, vol. 8, no. 6, pp. 6031–6037, 2014.

[23] F. Saurenbach, D. Wollmann, B. D. Terris, and A. F. Diaz, "Force microscopy of ion-containing polymer surfaces: morphology and charge structure," *Langmuir*, vol. 8, no. 4, pp. 1199–1203, 1992.

[24] K. Yatsuzuka, Y. Mizuno, and K. J. Asano, "Electrification phenomena of pure water droplets dripping and sliding on a polymer surface," *Journal of Electrostatics*, vol. 32, no. 2, pp. 157–171, 1994.

[25] K. Yatsuzuka, Y. Mizuno, and K. Asano, "Electrification of polymer surface caused by sliding ultrapure water," *IEEE Transactions on Industry Applications*, vol. 32, no. 4, pp. 825–831, 1996.

[26] Z. H. Lin, G. Cheng, L. Lin, S. Lee, and Z. L. Wang, "Water-solid surface contact electrification and its use for harvesting liquid-wave energy," *Angewandte Chemie International Edition*, vol. 52, no. 48, pp. 12545–12549, 2013.